



**HAL**  
open science

## Calculations of Auger intensity versus beam position for a sample with layers perpendicular to its surface

L Zommer, A Jablonski, Senoner M , Wirth Th, Unger W , Osterle W ,  
Kaiander I

### ► To cite this version:

L Zommer, A Jablonski, Senoner M , Wirth Th, Unger W , et al.. Calculations of Auger intensity versus beam position for a sample with layers perpendicular to its surface. *Journal of Physics D: Applied Physics*, 2010, 43 (27), pp.275301. 10.1088/0022-3727/43/27/275301 . hal-00569642

**HAL Id: hal-00569642**

**<https://hal.science/hal-00569642>**

Submitted on 25 Feb 2011

**HAL** is a multi-disciplinary open access archive for the deposit and dissemination of scientific research documents, whether they are published or not. The documents may come from teaching and research institutions in France or abroad, or from public or private research centers.

L'archive ouverte pluridisciplinaire **HAL**, est destinée au dépôt et à la diffusion de documents scientifiques de niveau recherche, publiés ou non, émanant des établissements d'enseignement et de recherche français ou étrangers, des laboratoires publics ou privés.

# Calculations of Auger intensity versus beam position for sample with perpendicular layers to its surface

L Zommer<sup>1</sup> and A Jablonski

Institute of Physical Chemistry, Polish Academy of Sciences, ul. Kasprzaka 44/52, 01-224 Warsaw, Poland

E-mail: zom@ichf.edu.pl

## Abstract

Recent advances in nanotechnology are a driving force for the improvement of lateral resolution in advanced analytical techniques such as SEM or SAM. Special samples with multilayers which are perpendicular to their surface are presently proposed for testing the lateral resolution, as discussed in recent works of Senoner et al (Senoner M, Wirth Th, Unger W, Osterle W, Kaiander I, Sellin R L and Bimberg D 2004 *Surface Interface Anal.* **36** 1423). The relevant experiment needs a theoretical description based on a recent progress in the theory. Monte Carlo simulations of electron trajectories make possible an accurate description of the considered system. We selected exemplary samples, with layers perpendicular to the surface. The layer materials are elemental solids with high, medium and low atomic numbers, i.e. Au|Cu|Au and Au|Si|Au. For these systems calculations of the Auger current versus beam position were performed. We found that, for system with layers consisting of elements of considerably different atomic numbers, the relation can have unexpected extreme. This observation can happen to be important in analysis of SAM pictures.

*PACS:* 72.10.-d;72.90+y

*Keywords:* Electron-solid interactions, elastic and inelastic scattering; Monte Carlo algorithm; Computer simulation; Continuous slowing down approximation; Backscattering yield; Auger current;

---

<sup>1</sup> Author to whom any correspondence should be addressed.

## 1. Introduction

Analytical applications of Auger electron spectroscopy (AES) require knowledge of a theoretical model that describes the Auger electron intensity emitted from a sample of a given structure. Well known application of AES is the determination of the surface composition from measured intensities of Auger electron signals. Another application of this technique is the measurement of the overlayer thickness. Under ion bombardment, we can measure the in-depth profiles of component element for non-uniform samples. However, a possibility of focusing the primary beam and scanning the surface opened an important application of determining the lateral elemental distribution on a surface (mapping). Scanning Auger microscopy (SAM) is particularly useful for analysis of non-uniform samples consisting of different chemical species.

An obvious parameter determining the resolution of SAM images is the diameter of the focused electron beam at the surface. In modern spectrometers, this diameter is below 10 nm which facilitates imaging of nanostructures at surfaces. The image may be affected by 3D structures at the surface which results in shadowing effect of electron recapture by surface protrusions. However, already in 1970s, it has been realized that the lateral resolution is also affected by the physical phenomena [1, 2]. The backscattered electrons may ionize surface atoms far from the point of a beam impact which is decreasing the image resolution. This effect is visualized theoretically by determination of the radial distribution of the points of electron exit (the point spread functions) (Cf. Ref. [3]). This issue has been recently addressed by Powell [4] and Jablonski and Powell [5]. New parameters were proposed to describe the radial distribution.

Lateral resolution of SAM may be determined experimentally, however this approach requires special reference samples. One of the samples that can be used for this purpose is the thin overlayer with a sharp edge [5]. We can determine then the “edge resolution” for a given spectrometer. Unfortunately, the measured signal, apart from the backscattering effects, is affected by the 3D structure of the surface region. The influence of the surface structure on the measured AES signal has been analyzed in detail by Tuppen and Davies [6].

A new type of the reference samples for testing the lateral resolution of surface techniques has been proposed by Senoner et al. [7, 8, 9] and Vila-Comamala et al. [10]. The sample is a multilayer system, with layers of known thickness. The surface submitted to analysis is perpendicular to the planar interfaces. In that case, one is avoiding the effect of the 3D structures since the surface can be plain. The authors proposed the layers of AlGaAs and InGaAs grown on the GaAs substrate as a reference [7, 8, 9]. Such sample can be used as a reference for different techniques, e.g. SIMS, and XPS. The authors also suggest usefulness of reference samples for AES [7].

In a recent publication, the Monte Carlo strategy was proposed for simulation of electron trajectories in a surface region of idealized samples with perfectly flat surface and perpendicular layers to their surface having infinitesimally thin interfaces [13]. Presently, we extend this model for calculating the Auger electron signal intensity during the primary beam scan perpendicular to the interfaces. We try to interpret the found unexpected extremes for investigated systems with layers filled by elements of considerably different atomic numbers, i.e. Au|Cu|Au and Au|Si|Au.

## 2. Theory

### 2.1. The Monte Carlo model

A solid is considered as a system composed of a number perpendicular layers to its surface of different materials, see example of such a structure in figure 1. The layers are homogeneous and amorphous throughout, in which the scattering centers are distributed randomly. The electron moving in the solid undergoes two independent processes: elastic and inelastic collisions. The latter events are described by the continuous slowing down approximation (CSDA). Within this approximation, an electron energy is a function of a distance traveled in a solid. According to the CSDA approximation the energy losses are described by the stopping power function (SP),  $S(E)$ , which is defined as the energy loss with respect to the path length,  $s$ :

$$S(E) = -\frac{dE}{ds} \quad (1)$$

If electron of energy  $E_1$  passes the distance  $s$  along its trajectory, then its energy decreases to  $E_2$ . New energy,  $E_2$ , can be calculated from the equation:

$$s = - \int_{E_1}^{E_2} \frac{dE}{S(E)} \quad (2)$$

Details can be found in refs [11] or [12].

The elastic scattering is considered as a series of straight segments. The end of each segment represents a random scattering event where new direction and new path length of the electron is set. Generation of a new scattering angle is described for example in ref. [11] and the way of generating the path length in layered sample in ref. [12].

The electron trajectory is followed from its entry point into the sample until it leaves the surface or its energy reaches the cutoff energy, i.e. the ionization energy,  $E_i$ , corresponding to selected Auger transition.

## 2.2. Auger current calculations

The formula for the Auger current [14],  $J_A$ , emitted into the unit solid angle of  $\alpha$  direction and coming from the analysed atoms in a uniform solid of density  $N$  (number of atoms in a unit volume) can be written as:

$$J_A(\alpha) = \frac{C}{4\pi} I_0 N \sigma(E_p) \sec\theta_0 r P_A \sec\theta_0 Q \lambda \cos\alpha \quad (3)$$

The symbols have the usual meaning:  $C$  contains spectrometer transmission and detector efficiency,  $I_0$  is the primary beam current,  $\sigma(E_p)$  is the ionization cross section of the level corresponding to the selected Auger transition for the incident energy  $E_p$ ,  $r$  is the backscattering factor (BF),  $P_A$  is the probability that the Auger transition follows the ionization,  $\theta_0$  is the incident angle of the primary beam,  $Q$  is a correction parameters accounting for the elastic scattering effects,  $\lambda$  is the inelastic mean free path (IMFP) and  $\alpha$  is the emission angle of the Auger electron with respect to the surface normal.

The formula properly modified can be used to describe Auger current for layered sample with layers parallel to its surface [12]. However, the aim of this paper is an attempt to determine the Auger

current emitted from the sample with perpendicular layers to its surface versus incident electron beam position. The question arises if the formula (3) can be used for such sample. For example, if an incident electron beam of energy  $E_p$  changes its distance,  $x$ , to the Si layer (see figure 1), the BF,  $r$ , may vary. Thus, to obtain  $J_A$ , assuming that eq. (3) applies to such sample, we should know the BF as a function of the electron beam position  $x$ . Besides, we can not exclude that the parameter  $Q$ , responsible for electron elastic scattering, also depends on  $x$ .

These difficulties encouraged us to look for the alternative in the problem solution. We propose the Monte Carlo (MC) simulation which makes possible to determine the Auger current versus the electron beam position which omits problem of the BF calculation. Although a theoretical description of the electron transport phenomena in a solid is now well-known, an algorithm applicable to samples with perpendicular layers to its surface has not been developed yet, with exception of a report devoted to a paradox of backscattering yield (BY) dependence on electron beam position for the same kind of samples [13].

We would like to express Auger current in such a way that can be adopted for other, more complicated, sample geometry. Since the ionizations efficiency and probability of Auger electron escape from sample depend on depth,  $z$ , we divide the sample into very thin layers  $\Delta z$ , parallel to the surface (we assume  $\Delta z=1\text{\AA}$ ). The number of ionizations in  $i$ -th  $\Delta z$  layer is proportional to sum of the products:

$$\sum_{j=1}^n \sum_{k=1}^{k_{j,i}} \sigma(E_{i,j,k}) s_{i,j,k} \quad (4)$$

where  $s_{i,j,k}$  is  $k$ -th segment from  $k_{j,i}$  segments of the  $j$ -th trajectory in  $i$ -th thin  $\Delta z$  layer within perpendicular layer of interest. Example in figure 2 shows an  $j$ -th trajectory which crosses an  $i$ -th  $\Delta z$  layer and has four segments in it within Si layer ( $k_{j,i}=4$ ) for a given transition.  $\sigma(E_{i,j,k})$  is a cross section for ionization of an atom by electron having energy  $E_{i,j,k}$  at the moment when it moves along segment  $s_{i,j,k}$ .  $n$  is a total number of generated trajectories. In our calculations we used the ionization cross section of Casnati et al [15].

The Auger electron signal is proportional to the following expression:

$$J_A(\alpha, x) = \frac{1}{n} \sum_{i=1}^T \left( \sum_{j=1}^n \sum_{k=1}^{k_{j,i}} \sigma(E_{i,j,k}) s_{i,j,k} \right) \varphi(i\Delta z, \alpha) \quad (5)$$

where  $\varphi(i\Delta z, \alpha)$  is the emission depth distribution function (DDF) for depth  $i\Delta z$ , and  $\alpha$  is the emission angle with respect to the surface normal. The DDF is a parameter typically used in the formalism of AES, and is defined [16,17] as the probability that Auger electron leaving the surface in a specified direction originated from a specified depth measured normally from the surface into the material.  $T$  is a number of  $\Delta z$  layers within information depth. We omitted here for clarity some constants such as the density of the analysed atoms in a solid, or the probability that the Auger transition follows the ionization. It is rather obvious that the Auger current,  $J_A(\alpha, x)$ , depends in general on beam position,  $x$ , since even the same trajectory as, for example, that one seen in figure 2, would cross the Si and Au layers differently if it was moved in  $x$  direction by some distance; in a result the number of trajectory segments in  $\Delta z$  layer merged in Si and their individual lengths as well their summary length would change in general.

Function  $\varphi$  was determined by MC simulations [11]. According to frequency concept of probability, function  $\varphi(i\Delta z, \alpha)$  should be a ratio of the number of Auger electrons leaving the sample into direction  $\alpha$  and produced in the thin layer  $\Delta z$  at the depth  $i\Delta z$ ,  $\Delta I(i\Delta z, \alpha)$ , to their total number created in the same layer  $\Delta z$ ,  $\Delta I_t(i\Delta z)$ :

$$\varphi(i\Delta z, \alpha) = \frac{\Delta I(i\Delta z, \alpha)}{\Delta I_t(i\Delta z)} \quad (6)$$

In our MC calculations Auger electrons are generated with a uniform distribution at a certain depth interval. They are assumed to be attenuated exponentially along the trajectory length in a solid. Thus, when an Auger electron represented by  $j$ -th trajectory generated at depth  $i\Delta z$  in thin layer  $\Delta z$  escapes sample with angle  $\alpha$ , its contribution to the Auger electron current, for multilayered sample having  $p$  material layers perpendicular to its surface, is

$$\Delta I(i\Delta z, \alpha) = \sum_{j=1}^{m_i} \exp \left[ - \left( \sum_{l=1}^p \sum_{k=1}^{k_l} \frac{d_{k,l,j,i,\alpha}}{\lambda_l} \right) \right] \quad (7)$$

where  $d_{k,l,j,i,\alpha}$  is  $k$ -th segment of the  $j$ -th trajectory in  $l$ -th perpendicular layer, starting at depth  $i\Delta z$  (starting within the material layer of interest), and emerging from sample in  $\alpha$  direction; the  $l$ -th perpendicular layer of material is crossed by the  $j$ -th trajectory  $k_l$  times;  $\lambda_l$  is the respective IMFP for a material filling the  $l$ -th perpendicular layer.  $m_i$  is a number of trajectories of Auger electrons generated in layer  $\Delta z$  at depth  $i\Delta z$ . Thus, it follows that

$$\varphi(i\Delta z, \alpha) = \frac{\sum_{j=1}^{m_i} \exp \left[ - \left( \sum_{l=1}^p \sum_{k=1}^{k_l} \frac{d_{k,l,j,i,\alpha}}{\lambda_l} \right) \right]}{m_i} \quad (8)$$

### 3. Results and discussion

In the MC calculations the total Auger electron emission current was determined; normal incidence of the beam on a sample has been assumed. The electron beam was assumed to have the diameter of 10 nm and the uniform cross-section. The calculated Auger signal intensity depends on number of factors, between them are, for example, probability of Auger transition, transmission function of the analyzer, detector efficiency etc. It is difficult to determine these factors thus the calculated Auger current intensities are presented in arbitrary units. Besides, we are not interested in absolute Auger signal values but in a shape of the signal versus beam position relation.

Figure 3 presents calculated relation of the Auger signal for Si 92 eV transition (99 eV – ionization energy) versus electron beam position,  $x$ , for the Au|Si(100nm)|Au system for electron primary energies,  $E_p$ , of 1, 2.5, 5, 10 and 25 keV. We see that the signal is not constant for the Si layer in general, as one could expected. For 5 keV beam energy the minimum is clearly seen, while the maximum is observed for 2.5 keV.

It seems worthwhile to see the relation for various Si layer thicknesses of the Au|Si|Au system. Figure 4 shows the results for the Si layer thicknesses of 30, 100, 200 and 500 nm for selected primary energy  $E_p=5$  keV. We see two minima for the Si layer of thickness 500 nm in contrast to the case of 100 nm.

Before we explain these results qualitatively let us see the relation for the system with element with atomic number larger than Si, between Au layers, for example for copper. Figure 5 presents the results for the Au|Cu(100nm)|Au system for primary energies of 2.5, 5, 10 and 25 keV for Cu 920 eV transition (933 eV – ionization energy). In contrast to the case of Au|Si|Au system, we see no minimum. Additionally in the relation for 5 keV energy we see the maximum. Figure 6 presents the same relation for various Cu layer thicknesses of 30, 100, 200 and 500 nm for the selected primary energy of 5 keV. We see that for thicker Cu layer the Auger current becomes constant, except beam positions at distances less than 50 nm from the Cu|Au interfaces where it decreases when the beam moves to the Au layer.

These results can be explained qualitatively. In ref. [13] we analyzed the dependence of the BY versus beam position for the Au|Si|Au and Au|Cu|Au systems. The BY is a the ratio of the total number of electrons emitted from the sample with energies greater than 50 eV to the total number of electrons incident at a given energy and angle of incidence [18]. We have found that, depending on the beam position, the BY can have values substantially lower or higher than those corresponding to elements composing the layered sample. This phenomenon is due to differences in the cross sections for electron elastic backscattering on atoms and SP of the elements filling the layers. One could suppose that for different beam positions on a given layer, for which the BYs differ, the corresponding Auger currents should also differ. The reason of such a conclusion is an expectation that the number of ionisations is large where BY is large, because large BY means large number of outgoing electrons which cause atom ionizations in surface region. One must remember however that one should account for only these backscattered electrons which have energy not less than the ionization energy,  $E_i$ , for the Auger transition of interest. It means that, we should consider the BY not for cutoff energy of 50 eV, but for the energy equal to ionization energy,  $E_i$ , for respective transition. Let us denote such a BY as a BYE to stress that it is the ratio of the total number of electrons emitted from the sample with energies greater than ionization energy,  $E_i$ , corresponding to Auger transition of interest, to the total number of incident electrons,  $N_i$ . Thus we can write the following

$$BYE = \frac{1}{N_t} \int_{E_i}^{E_p} N_s(E) dE \quad (9)$$

where  $N_s(E)$  is the energy spectrum of the electrons scattered on a sample. As far as we know, no analytical expression exists which enable the BYE calculations depending on layer thicknesses of a sample, electron beam position, etc. Thus the MC approach seems to be only reliable theoretical tool.

Let us first consider the Auger signal case of the Si 92 eV transition ( $E_i=99$  eV) for the Au|Si(100nm)|Au system for primary energies of 5 keV and 1 keV (see figure 3). For the first energy we observe in figure 3 a clear minimum, but for the second one the signal is practically constant on the Si layer. The corresponding BYEs are presented in figure 7a, and, to facilitate analysis, the related signals are in figure 7b. We see in figure 7a that the BYE on the Si layer for 5 keV (open circles) is smaller than the BYE for uniform Si (denoted by dash line) and maximum deviation reaches 33% at the middle of the layer. We believe that it should have consequence in decrease of ionization number in surface region, thus, in decrease of the Auger electrons. In fact, beam position for which the BYE reaches minimum exactly corresponds with the signal minimum. A different situation is for the case of 1 keV primary energy, because the BYE on Si layer (figure 7a, full squares) almost does not deviate from the BYE for uniform Si (denoted by solid line), except small distances from the Si|Au interfaces, equal or less than diameter of the electron beam (10 nm). It implies that the signal (figure 7b, full squares) is practically constant except mentioned small distances from the interface where the beam starts to enter the Au layer.

It is of interest to understand why for the primary energy of 2.5 keV the AES signal for Si 92 eV transition reaches maximum (see figure 3), in contrast to the signal case with primary energy of 5 keV when it reaches minimum. It is helpful to consider figure 8. In figure 8a, we see the BYE (for the cut-off energy equal to  $E_i=99$  eV) versus beam position for the Au|Si(100nm)|Au sample for primary energies of 2.5 keV and, to facilitate comparison, for 5 keV. Figure 8b presents corresponding Auger signals. We see in figure 8a that for the primary energy of 2.5 keV the BYE (open squares) behaves differently from the primary energy case of 5 keV (open circles). When the beam moves to the middle of the Si layer the BYE, for 2.5 keV case, increases (except small region of the beam diameter

dimension in vicinity of the Si|Au interfaces), then reaches maximum. In consequence the corresponding signal behaves similar (see figure 8b, open squares), and reaches maximum at the middle of the Si layer. One may say that the shape of the signal run on the Si layer reflects itself in the corresponding BYE.

It seems rather obvious that the Si 92 eV signal is also observed when the beam impinges at the Au layer, not too far from the Au|Si interface (see figure 3), since backscattered electrons in the Au layer may penetrate the Si one and cause its atoms ionizations. Thus, it is understandable that for higher primary electron energy slower decrease of the Si 92 eV signal on the Au layer takes place with the increase of the beam distance to the Au|Si interface. The higher primary energy means greater possibility of electron penetration from the Au layer into the Si one where it can bring about the Si 92 eV transitions. When analyzing such a AES image one may ask where there is position of the material interface. We propose tentatively the inflection point of the image as an approximate position of the interface.

Similar analysis as above can be performed for the case of the Au|Cu|Au system. For example, the fact that the Cu 920 eV signal for the primary energy of 5 keV (figure 5, open circles) has maximum but the signal Si 92 eV for the Au|Si|Au system (figure 3, open circles) for the same primary energy has minimum can be readily explained with the help of figure 9a. However, some comments may need differences in runs of the signals Si 92 eV for the Au|Si(500nm)|Au system (figure 4, stars) and Cu 920 eV for the Au|Cu(500nm)|Au system (figure 6, stars) at the same primary energy of 5 keV, because the former has two minima, the latter has no minimum. The Cu 920 eV signal, in contrast to the Si 92 eV one, diminishes when the beam incident on middle layer approaches the interface. Figure 9b presents the corresponding BYEs for the both signals versus the beam position. We see that Si 92 eV signal (figure 4, stars) is a reflection of the BYE run in the range of the Si layer (figure 9b, open circles), since the signal and the BYE are constant in the middle of the Si layer and when the beam approaches the interface it diminishes and then, after reaching the minimum, increases. The BYEs in figure 9b corresponding to Cu 920 eV signal (filled squares), and the Si 92 eV signal (open circles), although seem to be qualitatively the same, relate to substantially different

signals as is seen in figures 4 and 6 (stars). The reason that Cu 920 eV signal, in contrast to the signal Si 92 eV, has no minima becomes clear if we take into account details of its corresponding BYE in figure 9b (filled squares). In almost all beam positions on the Cu layer the BYE is constant apart from the beam distances to the interface less than about 50 nm where it diminishes approaching the interface (except distance less than beam diameter); in result the Cu 920 eV signal (figure 6, stars) behaves similar to the BYE. Though we see increase of the BYE on the Cu layer (figure 9a, full squares) when the beam approaches interface, in its close vicinity, we do not see subsequent increase of the corresponding Cu 920 eV signal since the BYE increase starts when the beam distance to the interface reaches values less than the beam diameter (10 nm). Thus only diminishing fraction of the beam generates signal; in consequence the signal diminishes.

#### **4. Conclusions**

We performed the MC simulation of electron transport for selected exemplary systems with layers perpendicular to the surface. The layer materials were elemental solids with high, medium and low atomic numbers, i.e. Au|Cu|Au and Au|Si|Au. For these systems the calculations of the Auger current versus beam position were performed. We found that, for system with layers filled by elements of considerably different atomic numbers, the relation can have unexpected extremes. This observation can turn out to be important in analysis of SAM pictures.

## References

- [1] Kirschner J 1977 *Appl. Phys.* **14** 351
- [2] El Gomati M M and Prutton M 1978 *Surf. Sci.* **72** 485
- [3] Briggs D and Seah M P (Eds) 1990 *Practical Surface Analysis*, John Wiley, Chichester, p. 243.
- [4] Powell C J 2004 *Appl. Surface Sci.* **230** 327
- [5] Jablonski A and C. J. Powell 2005 *Appl. Surface Sci.* **242** 220.
- [6] Tuppen G A and G. J. Davies 1985 *Surface Interface Anal.* **5** 235
- [7] Senoner M, Wirth Th, Unger W, Osterle W, Kaiander I, Sellin R L and Bimberg D 2004 *Surface Interface Anal.* **36** 1423
- [8] Senoner M, Wirth Th, Unger W, Osterle W, Kaiander I, R. Sellin R L and Bimberg D 2005 in: *Nanoscale Calibration Standards: Dimensional and Related Measurements in the Micro-and Nanometer Range*, Edited by G. Wilkening G and L. Koenders L, Wiley, Weinheim, p 21
- [9] Senoner M and Unger W 2007, *Surface and Interface Anal.* **39** 16
- [10] Vila-Comamala J, Jefimovs K, Raabe J, Pilvi T, Fink R H, Senoner M, Maaßdorf A, Ritala M and David C 2009 *Ultramicroscopy* **109** 1360
- [11] Zommer L and Jablonski A 2008 *J. Phys. D: Appl. Phys.* **41** 055501
- [12] Zommer L, Jablonski A, Kotis L and Menyhard M 2008 *J. Phys. D: Appl. Phys.* **41** 155312
- [13] Zommer L and Jablonski A 2009 *J. Phys. D: Appl. Phys.* **42** 195301
- [14] Jablonski A 1996 *Surf. Sci.* **364** 380
- [15] Casnati E, Tartari A and Baraldi C 1982 *J. Phys. B: At. Mol. Opt. Phys.* **15** 155
- [16] ISO 18115, *Surface Chemical Analysis - Vocabulary*, international Organisation for Standardisation, Geneva (2001); ISO 18115, *Surface Chemical Analysis - Vocabulary - Amendment 2*, International Organisation for Standardisation, Geneva (2007).
- [17] ASTM E673-03, Standard Terminology Relating to Surface Analysis, Annual Book of ASTM Standards 2006, Vol. 3.06, ASTM International, West Conshohocken, 2006, p. 647
- [18] ISO 18115 *Surface Chemical Analysis-Vocabulary*, International Organisation for Standardisation (2001), Geneva; Definitions of terms for surface analysis; definition 5.49

### Figure captions

**Fig. 1.** Example of the electron trajectory in a layered sample with layers perpendicular to its surface.

**Fig. 2.** Example of a  $j$ -th trajectory crossing a very thin  $\Delta z$  layer at depth  $i\Delta z$ . This trajectory has four segments in it ( $k_{j,i}=4$  within Si layer).

**Fig. 3.** Auger signal (Si 92 eV) versus electron beam position for the Au|Si|Au sample for various primary electron beam energies (a.u. – arbitrary units).

**Fig. 4.** Auger signal (Si 92 eV) versus electron beam position for the Au|Si|Au sample for various Si layer thicknesses for the beam energy of 5 keV (a.u. – arbitrary units).

**Fig. 5.** Auger signal (Cu 920 eV) versus electron beam position for the Au|Cu|Au sample for various primary electron beam energies (a.u. – arbitrary units).

**Fig. 6.** Auger signal (Cu 920 eV) versus electron beam position for the Au|Cu|Au sample for various Cu layer thicknesses for the beam energy of 5 keV (a.u. – arbitrary units).

**Fig. 7.** The BYE (a) and corresponding Auger signal (Si 92 eV) (b) vs primary electron beam position for the Au|Si|Au sample for the beam energy of 1 and 5 keV (a.u. – arbitrary units).

**Fig. 8.** The BYE (a) and corresponding Auger signal (Si 92 eV) (b) vs primary electron beam position for the Au|Si|Au sample for the beam energy of 2.5 and 5 keV (a.u. – arbitrary units).

**Fig. 9.** BYE corresponding to Si 92 eV and Cu 920 eV transitions versus primary electron beam position for Au|Si(100nm)|Au and Au|Cu(100nm)|Au systems (a), and Au|Si(500nm)|Au and Au|Cu(500nm)|Au systems (b) for the beam energy of 5 keV.

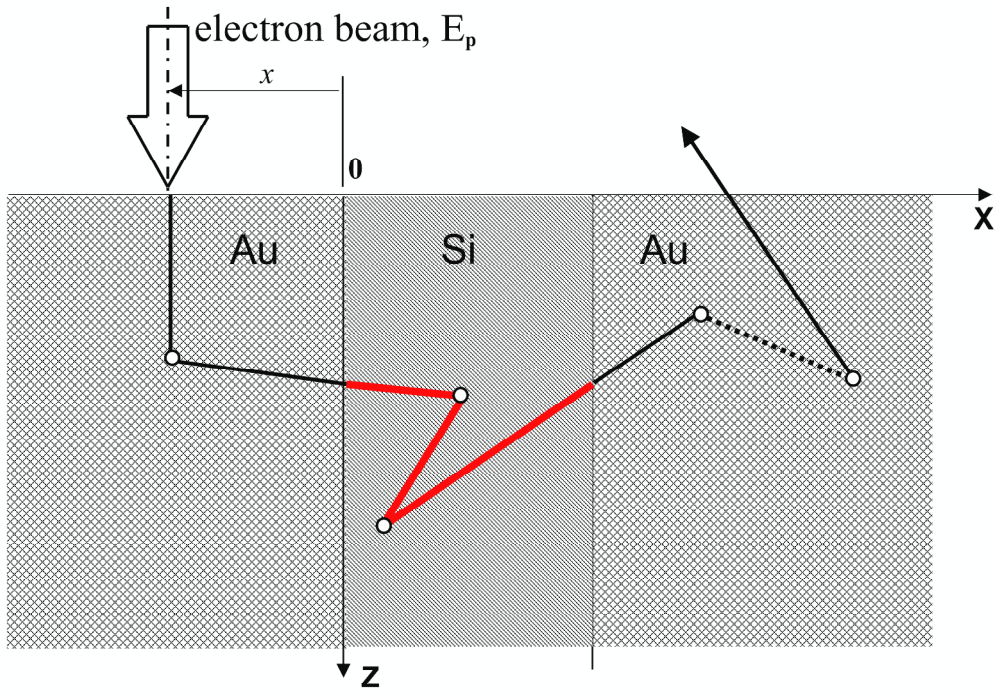


Fig. 1.

**Fig. 1.** Example of the electron trajectory in a layered sample with with layers perpendicular to its surface.

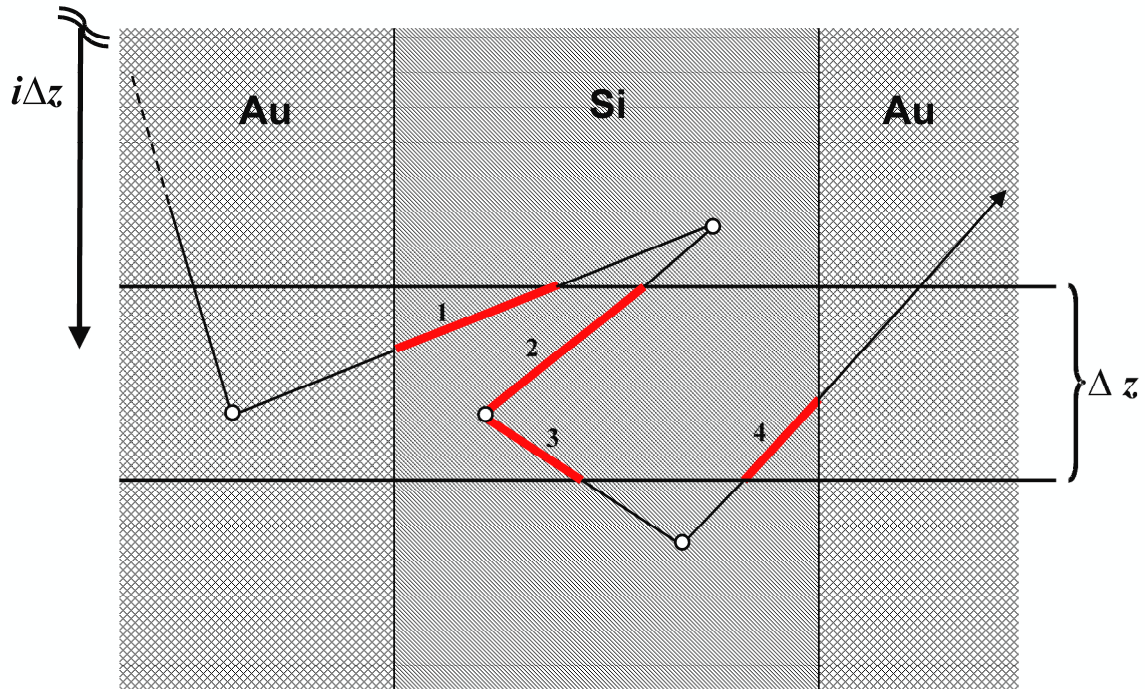


Fig. 2.

**Fig. 2.** Example of a  $j$ -th trajectory crossing a very thin  $\Delta z$  layer at depth  $i\Delta z$ . This trajectory has four segments in it ( $k_{j,i}=4$  within Si layer).

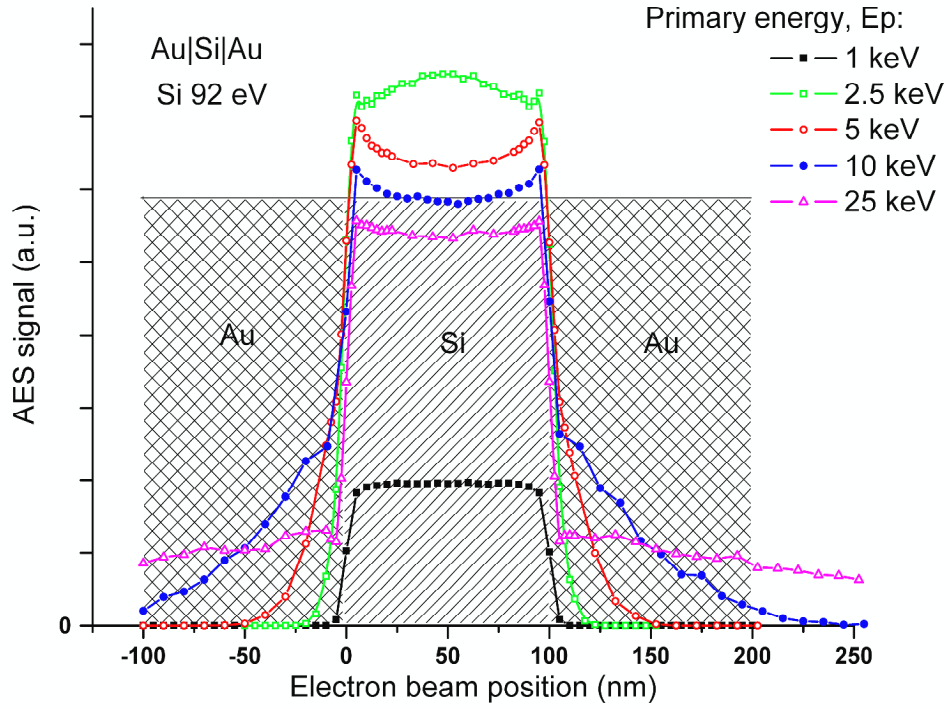


Fig. 3.

**Fig. 3.** Auger signal (Si 92 eV) versus electron beam position for the Au|Si|Au sample for various primary electron beam energies (a.u. – arbitrary units).

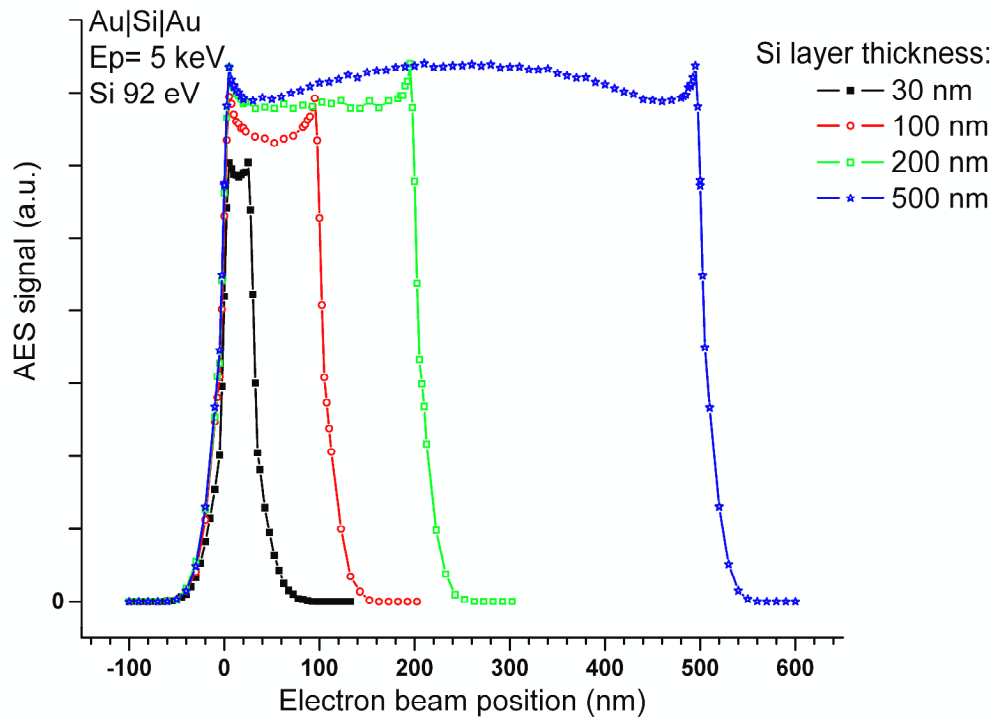


Fig. 4.

**Fig. 4.** Auger signal (Si 92 eV) versus electron beam position for the Au|Si|Au sample for various Si layer thicknesses for the beam energy of 5 keV (a.u. – arbitrary units).

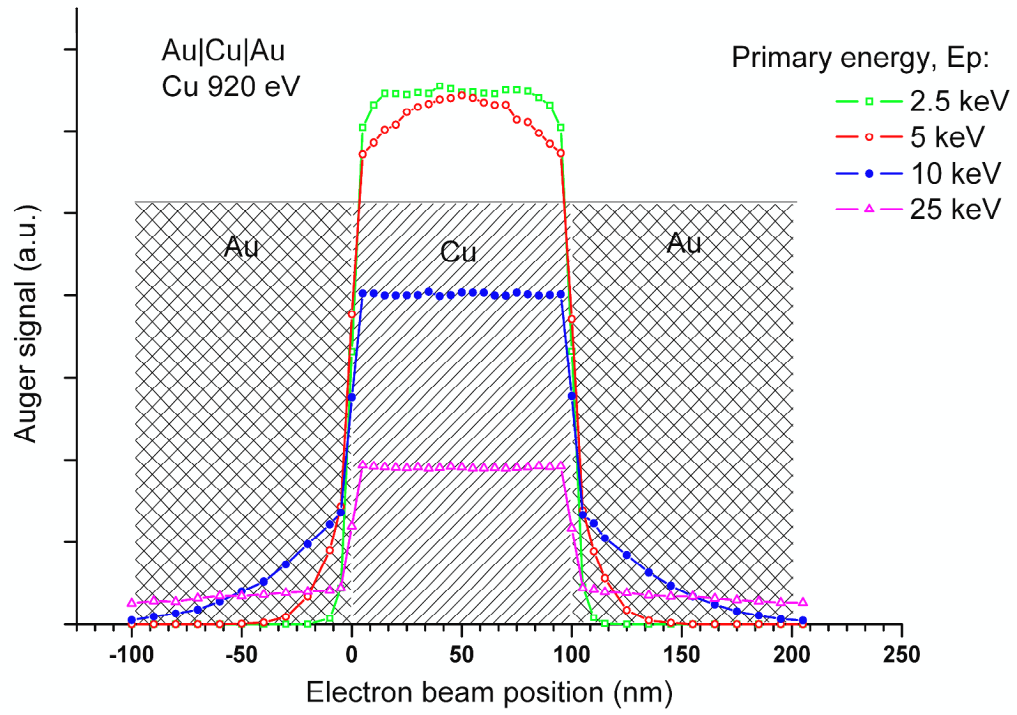


Fig. 5.

**Fig. 5.** Auger signal (Cu 920 eV) versus electron beam position for the Au|Cu|Au sample for various primary electron beam energies (a.u. – arbitrary units).

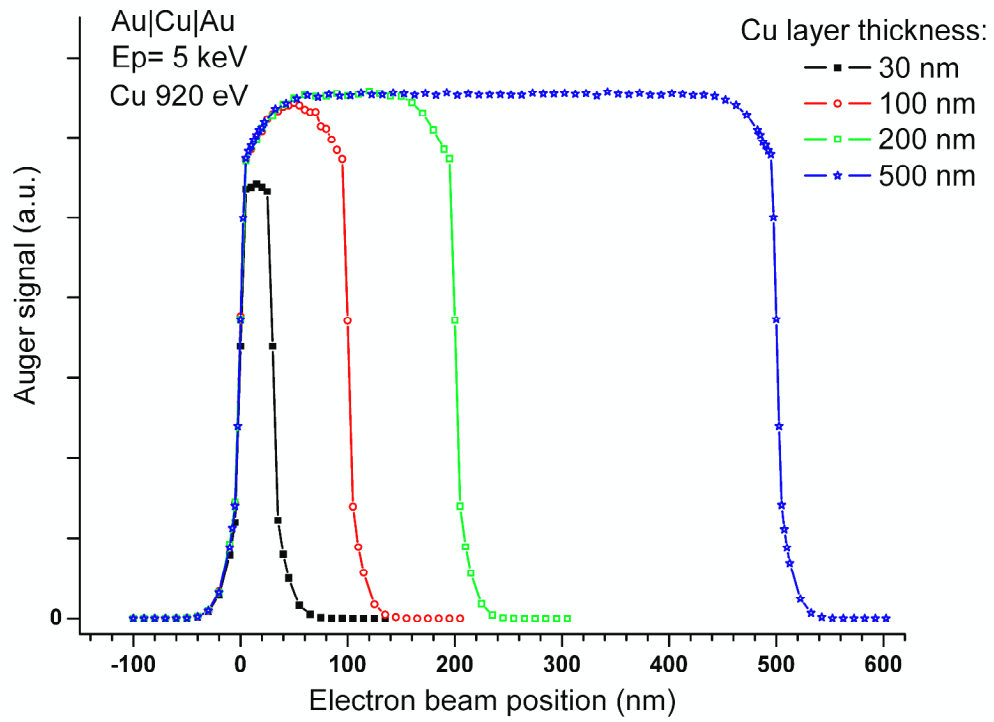


Fig. 6.

**Fig. 6.** Auger signal (Cu 920 eV) versus electron beam position for the Au|Cu|Au sample for various Cu layer thicknesses for the beam energy of 5 keV (a.u. – arbitrary units).

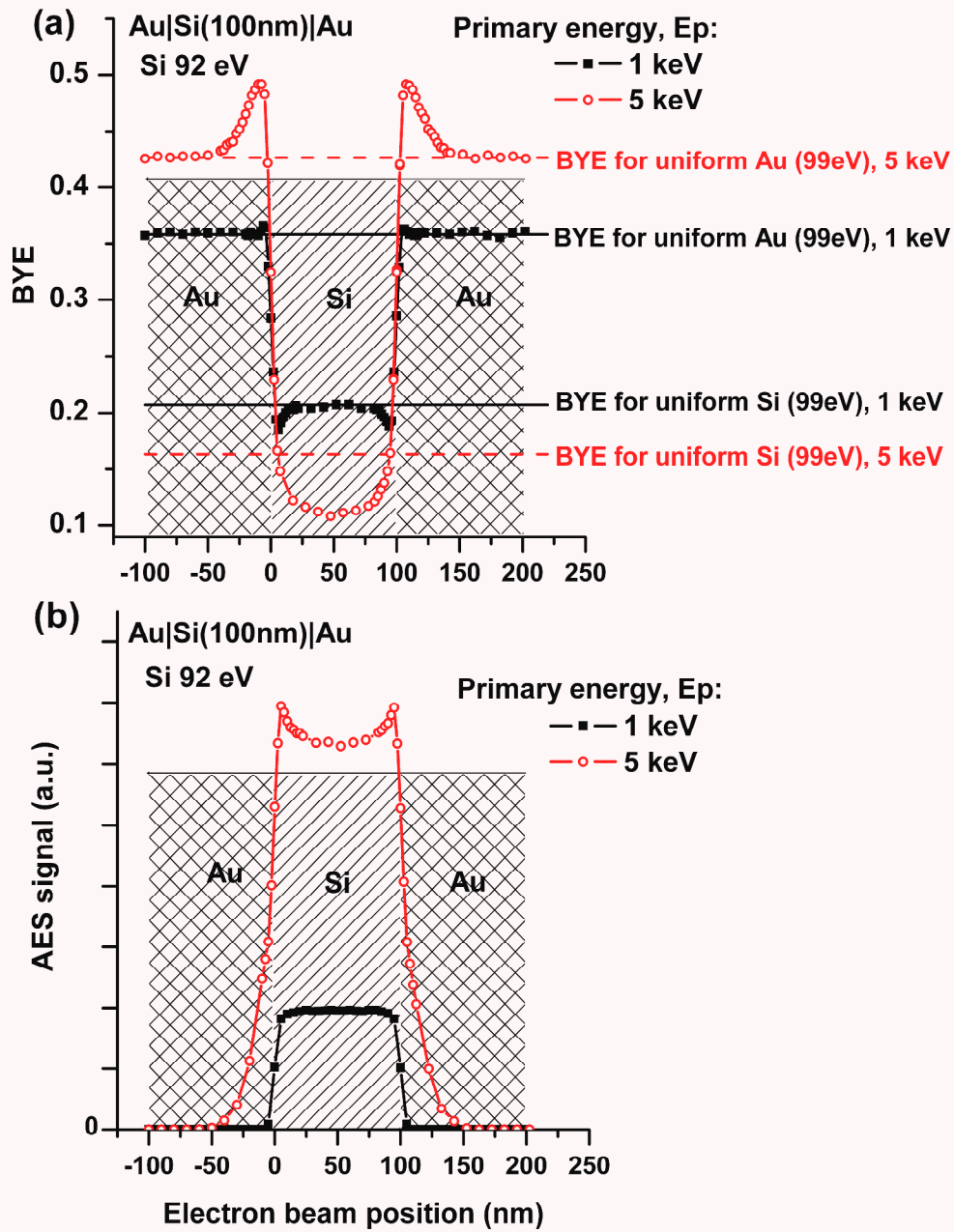


Fig. 7.

**Fig. 7.** The BYE (a) and corresponding Auger signal (Si 92 eV) (b) vs primary electron beam position for the Au|Si|Au sample for the beam energy of 1 and 5 keV (a.u. – arbitrary units).

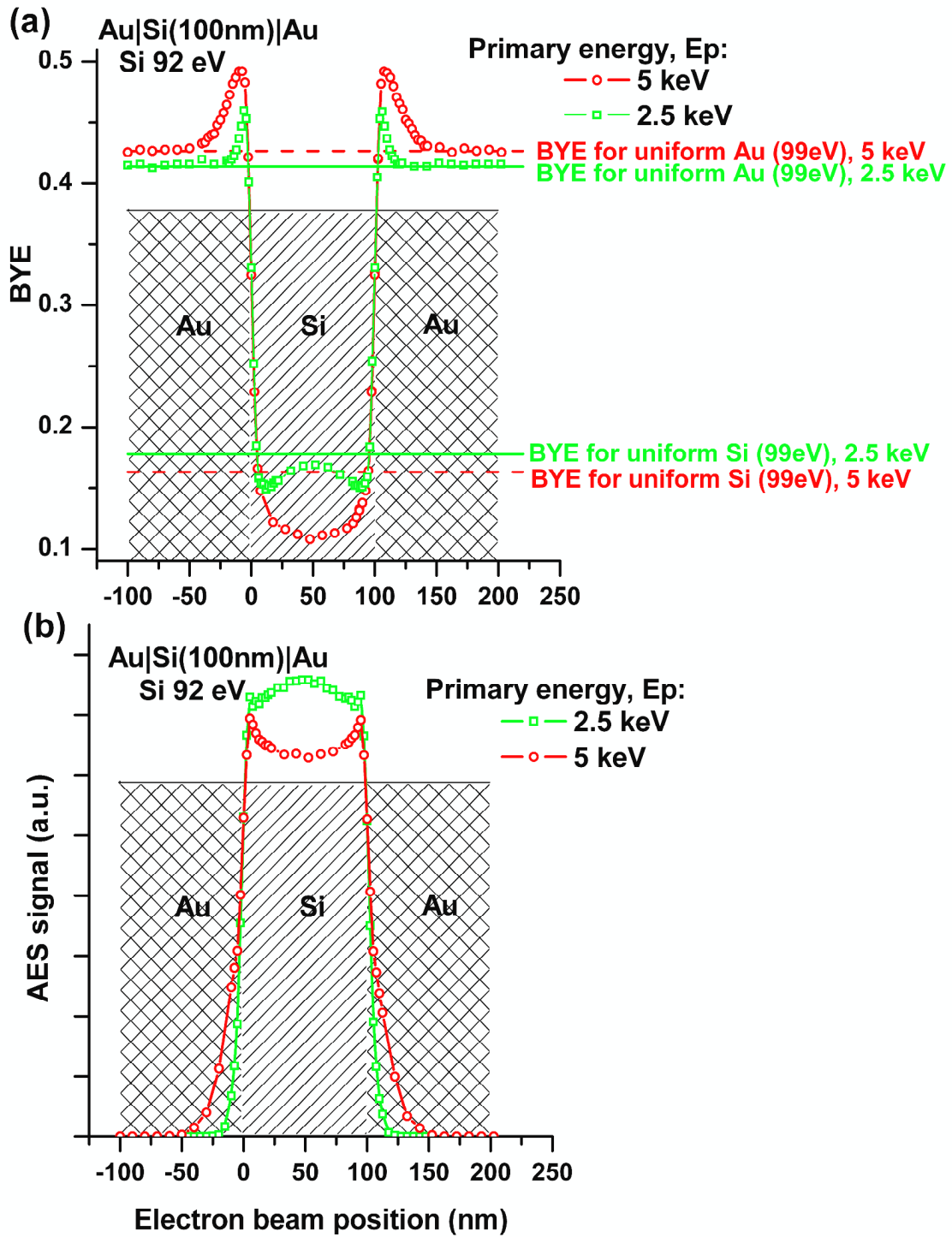


Fig. 8.

**Fig. 8.** The BYE (a) and corresponding Auger signal (Si 92 eV) (b) vs primary electron beam position for the Au|Si|Au sample for the beam energy of 2.5 and 5 keV (a.u. – arbitrary units).

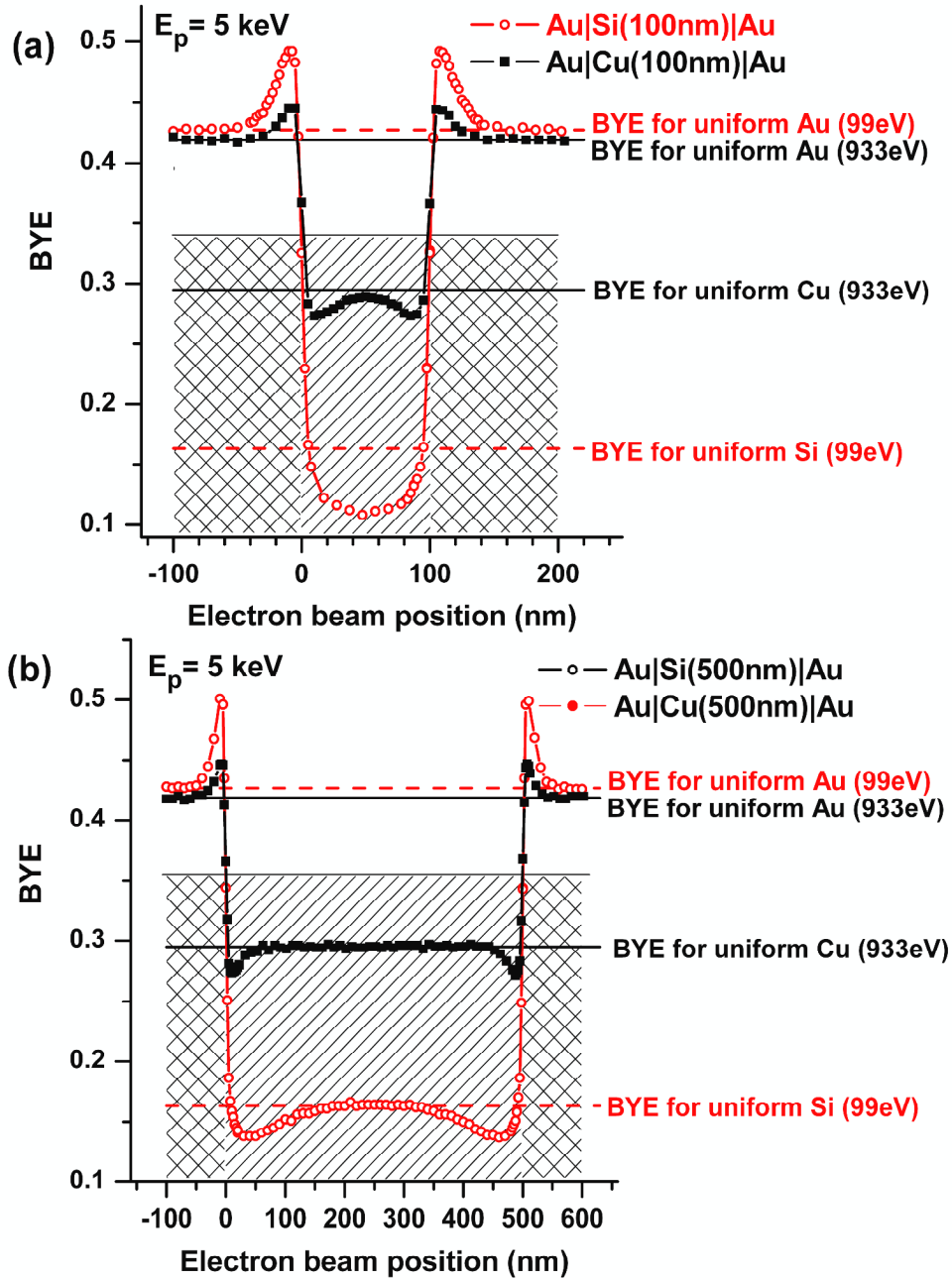


Fig. 9.

**Fig. 9.** BYE corresponding to Si 92 eV and Cu 920 eV transitions versus primary electron beam position for Au|Si(100nm)|Au and Au|Cu(100nm)|Au systems (a), and Au|Si(500nm)|Au and Au|Cu(500nm)|Au systems (b) for the beam energy of 5 keV.